NANO LETTERS

Letter

pubs.acs.org/NanoLett

Artificially Stacked Atomic Layers: Toward New van der Waals Solids

Guanhui Gao,[†,‡,#] Wei Gao,[§] E. Cannuccia,[∥,#] Jaime Taha-Tijerina,[†] Luis Balicas,[⊥] Akshay Mathkar,[†] T. N. Narayanan,[†] Zhen Liu,[†] Bipin K. Gupta,[¶] Juan Peng,[■] Yansheng Yin,[‡,*] Angel Rubio,[*,∥] and Pulickel M. Ajayan[*,†,§]

[†]Department of Mechanical Engineering and Materials Science, Rice University, 6100 Main Street, Houston, Texas 77005, United States

[‡]Institute of Materials Science and Engineering, Ocean University of China, Qingdao, China

[§]Department of Chemistry, Rice University, Houston, Texas 77005, United States

[∥]Nano-Bio spectroscopy group and ETSF scientific development centre, Departamento de Física de Materiales, Centro de Física de Materiales CSIC-UPV/EHU-MPC and DIPC, Universidad del País Vasco UPV/EHU, Avenida Tolosa 72, E-20018 San Sebastián, Spain

[⊥]National High Magnetic Field Lab, Florida State University, Tallahassee, Florida, United States

[¶]National Physical Laboratory (CSIR), Dr. K. S. Krishnan Road, New Delhi-110012, India

[■]School of Chemistry and Chemical Engineering, Nanjing University, China

S *Supporting Information*

ABSTRACT: Strong in-plane bonding and weak van der Waals interplanar interactions characterize a large number of layered materials, as epitomized by graphite. The advent of graphene (G), individual layers from graphite, and atomic layers isolated from a few other van der Waals bonded layered compounds has enabled the ability to pick, place, and stack atomic layers of arbitrary compositions and build unique layered materials, which would be otherwise impossible to synthesize via other known techniques. Here we demonstrate this concept for solids consisting of randomly stacked layers of graphene and hexagonal boron nitride (h-BN). Dispersions of exfoliated h-BN layers and graphene have been prepared by liquid phase exfoliation methods and mixed, in various concentrations, to create artificially stacked h-BN/G solids. These van der Waals stacked hybrid solid materials show interesting electrical, mechanical, and optical properties distinctly different from their starting parent layers. From extensive first principle calculations we identify (i) a novel approach to control the dipole at the h-BN/G interface by properly sandwiching or sliding layers of h-BN and graphene, and (ii) a way to inject carriers in graphene upon UV excitations of the Frenkell-like excitons of the h-BN layer(s). Our combined approach could be used to create artificial materials, made predominantly from inter planar van der Waals stacking of robust bond saturated atomic layers of different solids with vastly different properties.

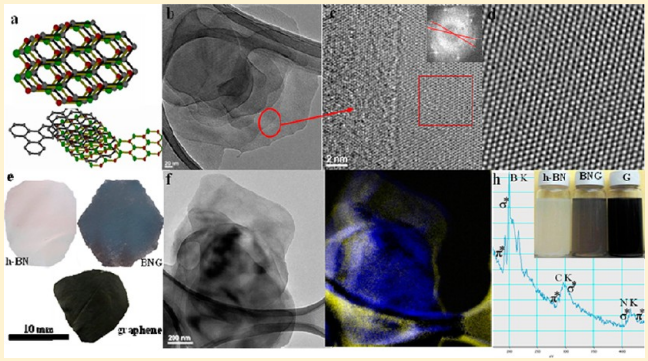

KEYWORDS: *van der Waal solids, hexagonal boron nitride (h-BN): graphene, exfoliation, artificial stacking: misfit layer, ab-initio, dipole, exciton*

There are several layered compounds, characterized by van der Waals forces between individual layers, such as graphite, h-BN, dichalcogenides, and so forth and the ability to extract individual layers from these solids have brought renewed interest in manipulating these materials.[1−4] Graphene (G), monolayer of graphite, has received enormous attention and has been formed by various techniques such as chemical exfoliation of graphite and vapor deposition.[5,6] Very recently, another layered compound, h-BN has also been exfoliated to obtain individual layers.[7] There is ongoing work to produce individual layers of dichalcogenides such as MoS_2 and WS_2.[8] It is possible to exfoliate atomic layers from these layered materials that span a broad range of properties. Electronically, graphene is semimetallic, h-BN is an insulator, and dichalcogenide layers have semiconducting properties. With the availability of these isolated atomic layers of various compositions and properties, there appears to be a unique opportunity to build artificially stacked (van der Waals) structures from layers of differing compositions and build hybrid materials by a simple solution self-assembly process. Layered solids of different materials containing van der Waals

Received: March 19, 2012
Revised: May 21, 2012
Published: June 25, 2012

   dx.doi.org/10.1021/nl301061b | *Nano Lett.* 2012, 12, 3518−3525

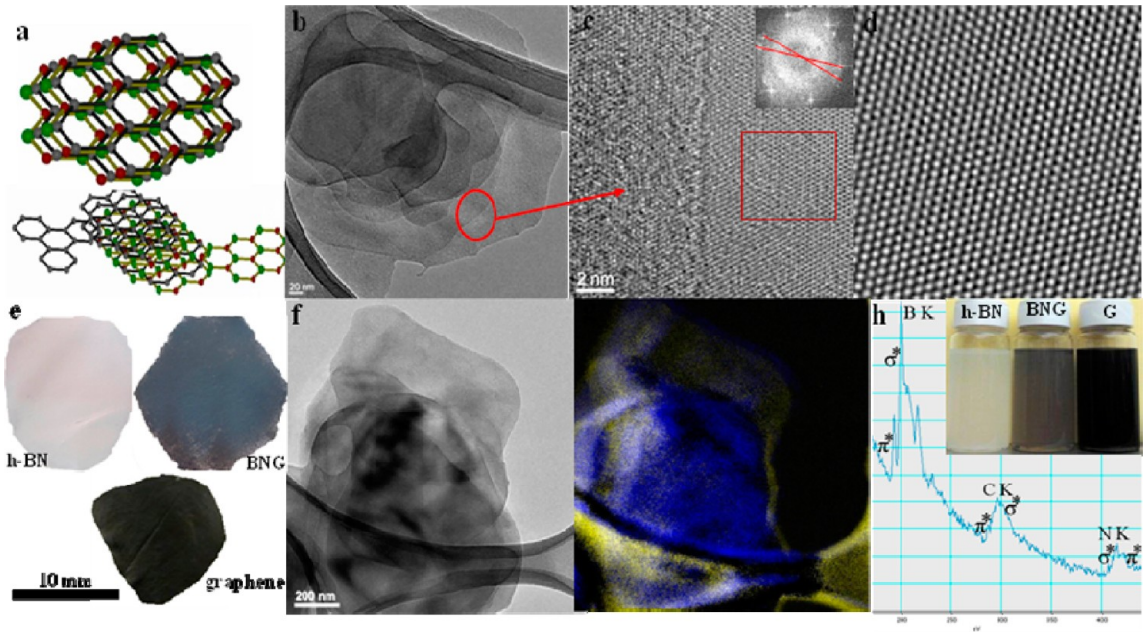

Figure 1. (a) h-BN and graphene hybrid nanosheets stack randomly. (b) Low-resolution TEM images of few-layer h-BN/graphene hybrid stacking prepared by mixing h-BN/IPA with graphene/DMF. (c) High-resolution TEM image of (b) at the edge, the FFT in the inset reveals two layers stacking with a relative rotational angle of 13°. (d) Individual atomic layers reconstructed by masking the FFT pattern from the area in image (c) (red line). (e) Free-standing films of h-BN, BNG hybrid, graphene. (f) The h-BN/GTEM image for mapping. (g) Boron mapping of image (f) and yellow color is graphene nanosheets; blue color is exfoliated h-BN nanosheets. (h) EELS spectrum of h-BN/graphene hybrid, K-shell excitations of B, C, and N.

gaps or noncommensurate layered compounds have been pursued in the past.[9−15] But synthesis of these materials in the past were mostly followed by multistage deposition techniques on substrates, limiting their large scale production. Here we demonstrate the concept of van der Waals solids and build extended solids, using two of the above-mentioned atomic layers, namely graphene and h-BN using a simple wet chemistry route. Moreover, both graphene and h-BN have in-plane bond saturation and chances of dangling bonds are limited. There have been a few previous attempts to fabricate graphene electronic devices on h-BN (considered as the best substrate for graphene[16]) and hybridized in-plane atomic layers containing h-BN and graphene. However, the synthetic method we report here can provide a generic approach to fabricate a variety of hybrid layered materials containing atomic layers of various compositions and properties. This detailed experimental analysis is further complemented with extensive first principle models that provide new microscopical insight allowing to identify the novel electromechanical properties stemming from these new heterostacked layers material.

It is well-known that solvents with low surface tension can be successfully used to exfoliate graphene and h-BN.[17−19] Several solvents such as *N*,*N*-dimethylformamide (DMF),[7] 1,2-dichloroethane(EDC),[20] poly(*m*-phenyl-enevinylene-co-2,5-dictoxy-p-phenylenevinylene)[21] have been reported for h-BN exfoliation. One may also exfoliate h-BN by using octadecylamine (ODA), amine-terminated polyethyleneglycol (PEG), Lewis-bases amine molecules with long lipophilic or hydrophilic chains.[22] However, these solvents are toxic and have a high boiling point, which makes it difficult to achieve large scalable production. Here, we exfoliate bulk h-BN and graphite powders using common solvents to yield single, double, few-layered h-BN nanosheets, graphene and then reassemble these as hybrid h-BN/G layered solids (see Supporting Information Figure S2 for more exfoliation details). According to the Hansen solubility theory,[23] parameters such as polarity, H-bonding, the cohesive energy density among others, are related to the effectiveness of the exfoliation process. Among these, surface tension is a key parameter.[17] Different solvents with strong enough surface tension to overcome the van der Waals forces of h-BN have been tested, and isopropanol (IPA) was selected to isolate h-BN because it can be easily removed after exfoliation. In addition, it is easy to scale up the exfoliation process with IPA and generate high-quality, layers of h-BN and graphene with yields of 10 wt %.

We can fabricate a hybrid film of h-BN and graphene nanosheets by mixing the exfoliated h-BN dispersion with that of graphene. In addition, different h-BN/G compositions in the film could be tuned by varying the volume ratio between each dispersion (see Supporting Information Figure S3), leading to a tunable band gap in the final hybrid films that may function well as semiconductors.[24] The proposed model for h-BN/G stacking hybrids could be clearly identified from detailed theoretical first-principles modeling. The stacking sequence is controlled by the interface dipole, which can be used to trigger the doping of a multilayer graphene and as a consequence of band gap opening. We believe that those h-BN and graphene nanosheets tend to stack alternately, offering a new and scalable heterostructure that cannot be made by any other techniques.

The h-BN and graphene nanosheets constitute our building blocks to produce extended solids as they assemble both laterally and in stacked direction to produce freestanding films. In our experiments, stacking of mono- and multilayered flakes were observed in low-resolution TEM images (Figure1b and Supporting Information Figures S1, S2). The lateral sizes of the exfoliated nanosheets range from 500 to 800 nm. The FFT pattern shown in the inset of Figure 1c indicates a 13° rotational angle between the two layers keeping the hexagonal

dx.doi.org/10.1021/nl301061b | *Nano Lett.* 2012, 12, 3518−3525

symmetry of the network. The h-BN/G nanosheets have an interlayer spacing of 3.356 Å (see Table1 and calculation detail

Table 1. Properties of Pure h-BN, Graphene, and Hybrids of h-BNG (1:1)

		Raman (cm^{-1})		
materials	XRD λ = 1.5418 Å	D	G	2D
h-BN	2θ = 26.74° d = 3.334 Å	1365		
Graphene	2θ = 26.34° d = 3.383 Å	1313.7	1581.3	2643.3
h-BN/G	2θ = 26.56° d = 3.356 Å	1325	1575	2661

in Supporting Information Figure S4), lying in between that of h-BN and graphite. The TEM mapping test (see Figure 1f, g) provides clear evidence that h-BN stacks on graphene layer by layer. In order to identify the atomic composition of the hybrid h-BN/G sheet, electron energy-loss spectroscopy (EELS) was performed. Figure 1h depicts the characteristic K-shell ionized edges of B, C, and N, corresponding to the edges at 189, 289, and 407 eV, respectively.[25−27] The visible edges of B, N, and C reveal the existence of one or more layers of graphene on top of h-BN (Supporting Information Figure S5). Therefore, the hybrid nanosheets are composed of both h-BN and graphene that are stacked alternately, but there is no long-range order along the thickness direction.

Further structural characterization is obtained by Raman spectroscopy with a 514.5 nm laser excitation. The pure h-BN signal is located at 1365 cm^{-1} (see Table 1 and Supporting Information Figure S6c),[28] whereas pure graphene shows characteristic G-peak around 1581.3 cm^{-1} (G) representing the in-plane bond-stretching motion of pairs of C sp^2 atoms, $E_{2\,g}$ mode. The 2D band is located at 2643.3 cm^{-1} corresponding to sp^2 atomic vibration,[29] and the D band at 1313.7 cm^{-1} indicates the graphene defect. For our new h-BNG hybrids, the G peak is located at 1575 cm^{-1} and the 2D peak at 2661 cm^{-1} with a broad band centered at 1325 cm^{-1}, probably due to the overlap of the D band of graphene and the 1365 cm^{-1} band in h-BN (Supporting Information Figure S6). Figure 2a,b show h-BN/G flakes but in different stacking orders, respectively, in Raman mappings at both 1580 and 1370 cm^{-1}, showing the distribution of graphene and h-BN, with a size of 10 μm × 10 μm (400 spectra in total). According to the mapping information, graphene is atop h-BN in the left region and h-BN is atop of graphene in the right region, as the arrows mark (more explanation in Supporting Information Figure S6e).

Thermal gravimetric analysis (TGA) showed a significant drop in mass starting at 678.9 °C, which is attributed to the combustion of graphene sheets in air, and the same phenomena was observed on the hybrid (Figure 2c), while h-BN is quite stable even beyond 800 °C. From the TGA curve, the ratio of h-BN/graphene in this hybrid is calculated to be 3:1. We demonstrate a solution based self-assembling approaches to achieve a layered solid hybrid of h-BN and graphene. This hybrid seems to be stable and forms small interlayer polar bonds to make the system stable.

After characterizing structurally our new-stacked solid, we address the optical properties of this material.[30−32] We first look at the ultraviolet−visible absorption spectrum shown in Figure 2d. The adsorption edge of exfoliated h-BN is located at 236 nm, which corresponds to an optical band gap of 5.26 eV. The band gap of h-BN varies according to fabrication methods and its hexagonal defects. In our study, it also depends on the stacking structures. Optical band gap measurements using Tauc formula may have its own limitations due to the resolution of the spectrum, leading to the band gap of pure h-BN appearing to be lower than theoretical result (about 6.0 eV). Extended sheets of h-BN/G hybrid were produced by filtration of the mixed dispersions by varying the volume ratio between each material, leading to tunable band gaps in the final h-BN/G hybrid (see Figure 2e and Supporting Information Figure S3 for the details on the calculations).

In Figure 3a−c, we show the measured XPS spectra of B, N, and C, respectively, from h-BN/G stacked solid. The main peak

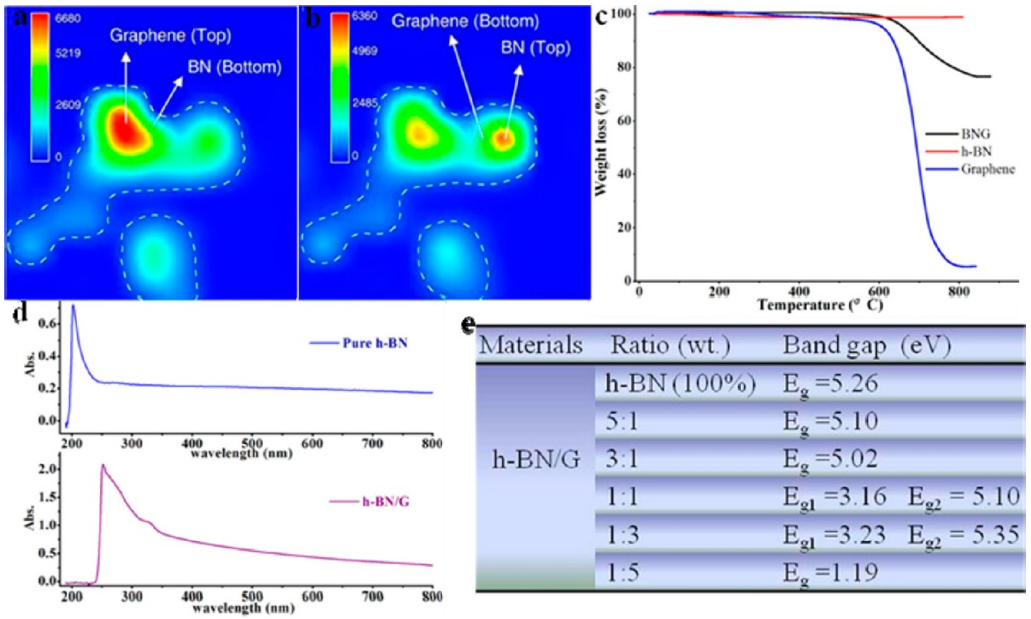

Figure 2. Evidence for a hybrid structure composed of h-BN and graphene. (a,b) Raman mapping of G/BN flakes. (a) Mapping at 1580 and (b) 1370 cm^{-1}. (c) TGA spectrum of graphene, hybrid of h-BN/G, h-BN. (d) UV−vis spectra of h-BN and hybrid of h-BN/graphene (3:1), respectively. (e) Band gap of hybrid of h-BN/G by different ratio between h-BN and graphene.

dx.doi.org/10.1021/nl301061b | Nano Lett. 2012, 12, 3518−3525

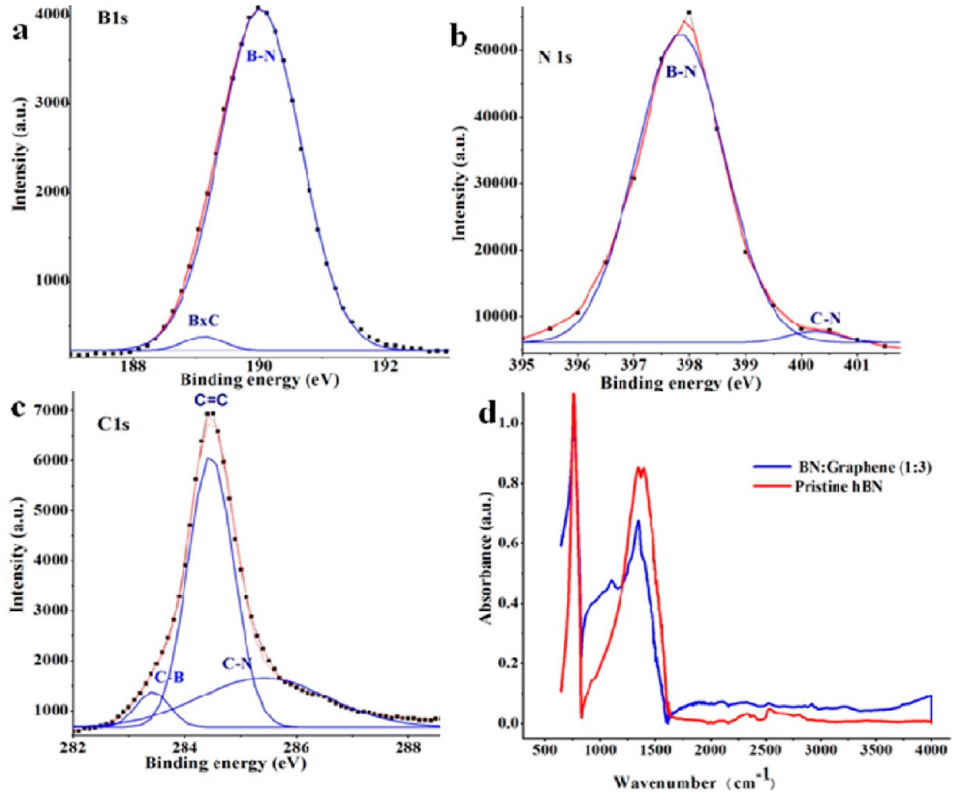

Figure 3. Evidence for h-BN/C hybrid. (a–c) XPS spectra of B, N and C 1s core levels, respectively. The spectrum curves (filled diamonds) are deconvoluted (blue curves) by Gaussian fitting (red curves), indicating possible multibonding information. (d) ATR-FTIR spectra of exfoliated h-BN and h-BN/G hybrid (1:3). Characteristic peaks at 760 and 1362 cm^{-1} corresponding to in-plane and out-of-plane are observed in the h-BN spectrum (red). In the hybrid h-BN/G spectrum, a feature at ~1101 cm^{-1} is observed in addition to the peaks at 760 and 1360 cm^{-1}.

of the B 1s spectrum is at 190.1 eV corresponding to the B 1s in h-BN.[33] This indicates that B is mainly bonded to N, like in h-BN where three N atoms are surrounding one B atom. But there can be a small shoulder peak around 189 eV, contributing to the broadening of the B 1s spectrum and which indicates a possible B_xC bonds in h-BN/G.[34] Polar covalent bonds between C atoms B atoms are possible due to their small difference in electronegativity.[5] This has been further confirmed by C1s spectrum and FT-IR (Figure 3d). N 1s spectrum is shown in Figure 3b and it also proclaims that the main bonding is between B and N corrensponding to a peak at 398 eV. A shoulder peak at higher energy (400.5 eV) is evidence from the spectrum and it indicates that N atoms partially bond with C atoms.[5] The C1s spectrum has a peak at 284.4 eV corresponding to that of graphene domains (indicated by C═C in spectrum) in h-BN/G. It also has shoulder peaks at lower binding energy and higher binding energy. The peaks at lower binding energy indicate the presence of C–B bonds (in agreement with Figure 3a) and the peak at higher binding energy shows the presence of C–N bonds as evidenced from Figure 3b. In conclusion, XPS and FT-IR spectra studies indicate that the solid has mainly bond-saturated planes but small amounts of possible out-of-plane chemical bonds could exist due to the dangling bonds created in the planes and broken edges during synthesis.

The attenuated total reflection Fourier transform infrared spectra (ATR-FTIR) of h-BN is shown in Figure 3d. It has two characteristic sharp features, one peak at 760 cm^{-1} indicative of in-plane bending vibration due to B–N, while another sharp peak at 1362 cm^{-1} that is characteristic of the out of plane vibration. In the h-BN/G hybrid, both peaks observed in the h-BN spectrum are observed, providing confirmation that the h-BN structure is undisturbed. An additional feature at 1101 cm^{-1} is also observed, the FTIR spectrum of graphene shows a number of peaks, but no clear feature at 1101 cm^{-1}(see Supporting Information Figure S7b),[35] which attribute this peak to the icosahedral structure of B_4C, while other studies[36] suggest the formation of boron carbide (B–C) bonds, resulting in IR absorption at 1100 cm^{-1}. While there is still a disagreement regarding the specifics of the chemical environment of the B–C bond, it is evident that there is chemical interaction between these stacked h-BN/G layers, which is resulting in the formation of amorphous B_xC bonds, leading to the absorption feature at 1100 cm^{-1}.

Since graphene and h-BN have very different electronic properties, every combination of (n)h-BN/(m)-G layers sequence exhibits specific properties dictated by the stacking of graphene (and h-BN) layers at the h-BN/graphene interface and the number of h-BN and G layers. In order to get more insight about the electronic properties of these new stacked structures, we performed extensive first principle density functional theory (DFT) simulations to determine their electronic and structural properties. Moreover, the optical response and the excited states have been computed using the state of the art of many body perturbation theory based on the previously computed DFT ground-state wave functions and eigenvalues (see Supporting Information Figure S8 for the details of calculations).[37,38] We advance the main two points stemming from the calculation: (i) those new structures open the possibility of mechanically controlling the electronic dipole

dx.doi.org/10.1021/nl301061b | Nano Lett. 2012, 12, 3518–3525

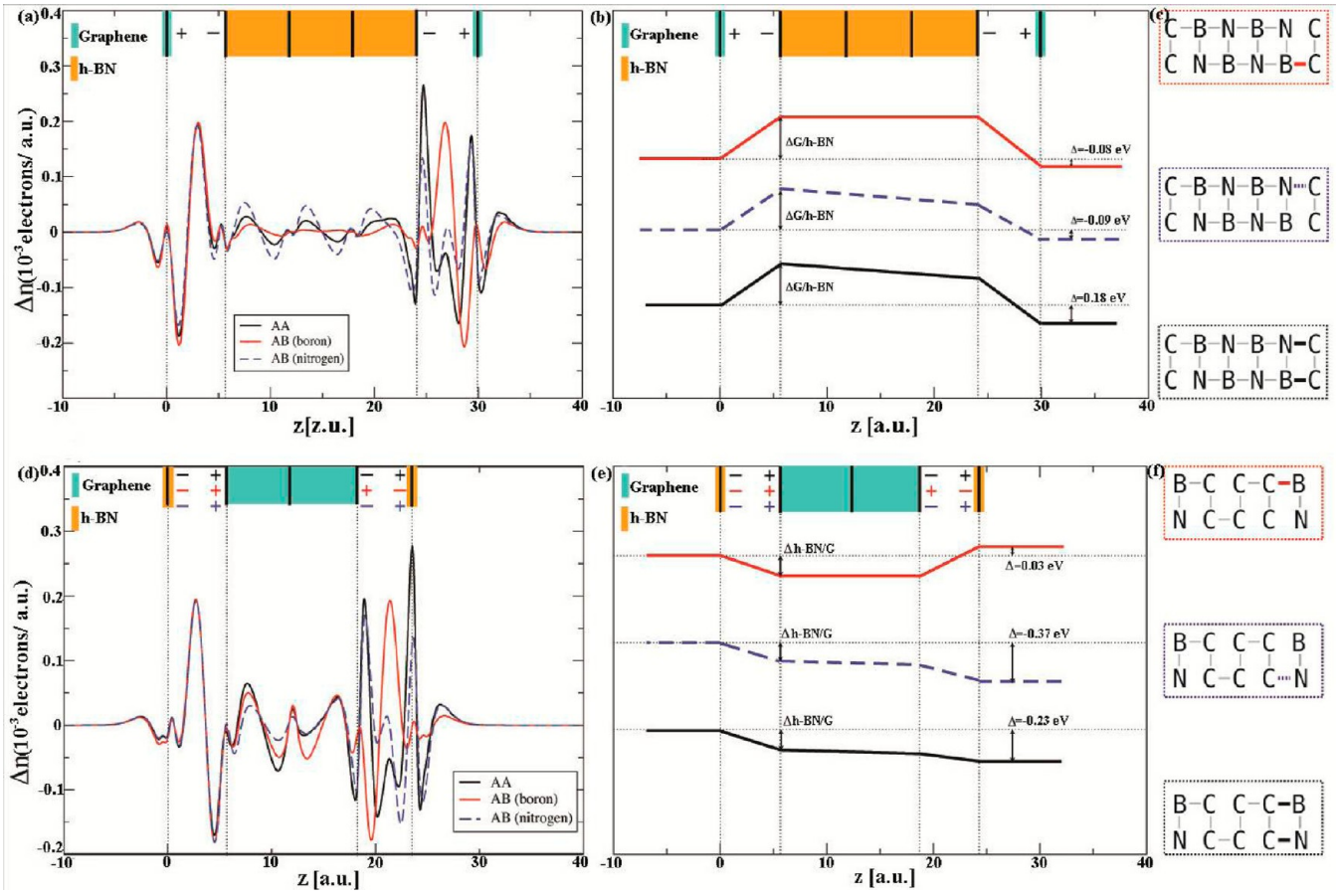

Figure 4. (a) and (d) Plane integrated electronic density difference for a G|4 layers h-BN|G and for a h-BN| trilayer G|h-BN hetero stacked structure respectively. The position of the top and the bottom layer of each substrate is indicated by a vertical dashed lines. In (a) and (d) we keep fixed the AB (boron) stacking at the first G/h-BN and h-BN/G interface respectively and we change the stacking at the interface of the opposite side of the slab. (c) and (f) Network representation of the slab stacking. A consistent use of colors in the network representation and both to plot and label the curves has been chosen to guide the eye (black for the AA stacking, red for the AB (boron) stacking and blue for the AB (nitrogen) stacking). (b) and (e) Schematic representation of the electrostatic potential profile across the slab.

at the h-BN/G interface and as consequence the electronic doping of the graphene surface; (ii) we identify a new charge injection mechanism to provide carriers in graphene though the optical excitation of the h-BN by UV photons. We should mention that the calculation imposes a commensurate configuration between the G and h-BN layers; this leads to the appearance of a small band gap (tenths of millielectronvolts) in graphene as reported by other works.[39] However, for the discussion below the presence of that small gap is irrelevant and, moreover, there is evidence that the incommensurability of the layers tends to wash-out that small gap opening.[40] The results presented here are in a different energy scale.

To illustrate the basic idea behind those new phenomena, we first look at the possibility of having different interfacial dipoles and whether or not those can be controlled by the stacking sequence.

We should mention that a similar idea was used to dope graphene layers that are supported on a thin film of h-BN/Cu(111).[39] First we want to address the question of whether we can have two different dipoles at two h-BN/G interfaces, if so we can have a distinct and different electrostatic doping of graphene via the insulating h-BN film. To assess this idea we designed a heterostructure sandwiching four layers of h-BN with graphene (see Supporting Information Figure S8a; note that the results could be generalized to graphite/4-h-BN/graphene and other stacked configurations but to illustrate the physics it is best to look at this graphene/4 h-BN/graphene). Before discussing the results let us fix the notation presented schematically in Figure 4c and 4f by link-network diagrams.

We have up to three different h-BN/G stacking sequences that mimic the AB and AA graphite stackings. Namely, AA stacking corresponds to an exact positioning of all C atoms on top on B and N atoms, and this is indicated by full links between C, B and N atoms; AB stacking indicates the case where one C atom is above the center of the h-BN hexagon and the other on top of the nitrogen atom, that we denote as AB (nitrogen) or over the boron, denoted as AB (boron). The h-BN stacking sequence is the usual AA', with B and N of one layer respectively on top of N and B of the layer below. In Figure 4a, we fix the left G/h-BN stacking to AB (boron) and we slide the other graphene in order to produce three different stacking sequences (sketched in figure 4c). Changing the stacking sequence from AA to AB (nitrogen) changes the concentration of electrons at the interface: it increases or decreases with respect to the quasi symmetric configuration (AB (boron) stacking at both the interfaces). The quasi symmetry comes from the fact that the two interfaces are the same but the two graphene layers are shifted one respect to the other. This is due to the AA' h-BN stacking and to the even number of layers composing the h-BN substrate. An odd

dx.doi.org/10.1021/nl301061b | Nano Lett. 2012, 12, 3518−3525

number of layers and the same h-BN/G interface would have led to a symmetric configuration. In Figure 4a we observe that the interface between graphene (G) and h-BN has an intrinsic dipole that comes from the work function mismatch and Pauli exchange repulsion that leads to interface charge rearrangement (see Figure 4b). One would expect this dipole to be equal on both G/h-BN interfaces; however as shown in Figure 4a this is not the case and it is a clear manifestation of the role of the crystallographic stacking sequence that is usually neglected. In fact, this phenomenon has been used previously[41] to tune the band gap of trilayer graphene. This stacking-induced dipole asymmetry can be used to control the doping of the h-BN/G interface (on the right), without resorting to any external field, rather exploiting the length of the h-BN. As the size of the h-BN buffer film increases, the electrostatic potential drops because of the charge difference at both ends of h-BN and moves the average effective potential acting on the second h-BN/G interface toward lower energies. This corresponds to an effective electron doping of the graphene, the amount of doping is linked to the length of the h-BN layer (see Supporting Information Figure S9b). We should mention that the saturation is reached by increasing the number of h-BN layer, as shown here. This idea can be extended to configurations in which instead of graphene we use a real noble metal like Cu or Au in order to induce a large variation of the dipoles and induced fields (and consequently of the doping level).

A second aspect of the same physical process discussed above would be the creation of an effective electric field through multilayer graphene. This has some nice implications for the case of trilayer graphene that if grown in ABC stacking exhibits a tunable gap by applying an electric field.[42] The simplified model to illustrate this idea consists of a trilayer graphene sandwiched with h-BN (depicted in Supporting Information Figure S8b) we use different crystallographic stacking sequences at both ends to induce an asymmetric dipole (see Figure 4d) and therefore an effective (small) field across (see Figure 4e). This is done in practice by changing the G/h-BN stacking sequence from AB (boron) to AB (nitrogen) or AA, while the G/h-BN interface is kept fixed as AB(boron). The results plotted in Figure 4e show that the right effective potential can be either above or below the left one depending on the stacking. The control of the dipole interface paves the way to several possible technological applications: the possibility to control the electrostatic doping and to convert mechanical energy into electrical one. A simple process of sliding the last layer induces a change in the potential and electrostatic doping. This effect depends on the underlying hybrid-stacked heterostructures.

After having discussed the change of the electronic properties induced by playing with the crystallographic stacking, we address now the optical properties. We know h-BN is characterized for having a strong Frenkel-like exciton around 6.1 eV and an onset of the absorption at about 5.8 eV[43] that is far from the main absorption region of graphene.[44] Then we expect interesting mixed excitonic states in our heterostructures. In fact, this is the case. The calculated optical absorption spectrum of a solid composed of alternated h-BN/G layers with ratio 1:1 and 3:1 is shown in Figure 5a. The analysis of the excitonic wave functions reveals that in the 1:1 case each exciton in the 3−6 eV region is composed by electronic transitions from nitrogen to the C−C bond of graphene. The excitonic wave function for those main peaks is characterized by having the electron mainly localized on the graphene layer if the

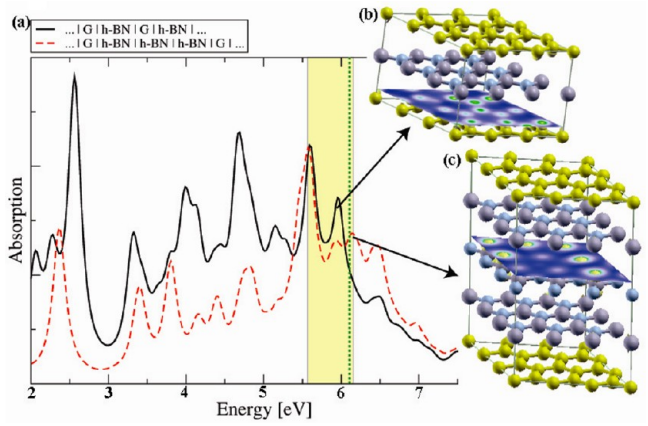

Figure 5. Optical absorption spectra of a solid composed of alternated graphene and h-BN layers in the ratio 1:1 (solid dark line) and 1:3 (dash red line). (a) We show the results of the GW+Bethe−Salpeter approach, and both lines are calculated with a broadening of 0.1 eV. The light polarization is parallel to the layers. The optical gap value position of the h-BN solid is marked by a green vertical dotted line.[39] The excitations of the 1:1 case (b) have a mixed nature, when the hole is localized on the h-BN layer the electron is on the graphene. In the 1:3 case (c). the excitations start to be localized on the h-BN layers; the energy region where this happens is inside the shadowed region.

hole is on the N of the h-BN layer, as shown in Figure 5b. The lower energy excitations are mainly localized on the graphene layer and have negligible contributions from the h-BN.

On the other hand in the 3:1 case the exciton at 6.11 eV is mainly localized on the h-BN layer, as Figure 5c shows. The excitons in the shadowed energy region drawn in Figure 5a have a pure character whereas the excitations below have a hybrid character. The presence of an exciton localized on the central h-BN layer in the 3:1 case is due to the fact that a larger number of h-BN layers reduce the metallic-like screening introduced by graphene when compared to the 1:1 case. In the limit of an infinite number of h-BN layers, the position of the bound exciton approaches the h-BN bulk value of 6.1 eV from below.[45] In the 1:1 case, the screening exerted by graphene is higher causing a redistribution of the well-defined unique excitonic peak of h-BN into several less intense excitons with a "mixed" nature. So the Frenkel nature of the h-BN exciton is modified and the exciton spreads over the surrounding graphene layers as Figure 5b clearly shows. Those results open the possibility of using the BN-layers as optical active device in the UV that can inject charges in the carbon layers by the direct excitation of the exciton of the h-BN.

In conclusion, here we demonstrate a new synthetic approach toward building solid materials from stacking of atomic layers from layered structures having wide range of properties. Here such a solid is constructed from layers of conducting graphene and insulating h-BN. The chemical exfoliation technique and mixing approach we have used here results in random stacking of layers in both lateral and thickness directions. However, layer-by-layer deposition techniques could be used to build more ordered stacks although getting alternating stacking of monolayer over large thicknesses could be conceptually feasible but would need long time. The concentration of each composition could be also tailored by using appropriate concentration of layers in the assembly; in our study, we created h-BN/G films with varying concentrations of h-BN and G. The approach we have reported here

dx.doi.org/10.1021/nl301061b | Nano Lett. 2012, 12, 3518−3525

allows for the formation of different hybrid materials built from 2D building blocks of various compositions, through their van der Waals stacking, assembled via a simple chemical route. Such materials could have fascinating properties due to the large number of interfaces between electronically dissimilar, flat, atomic layers bound through weak van der Waals forces. In fact, we have shown how the crystallographic stacking introduced a new order parameter that controls the interfacial dipoles and therefore the effective electrostatic doping of the surfaces.

■ ASSOCIATED CONTENT

Supporting Information

Additional information and figures. This material is available free of charge via the Internet at http://pubs.acs.org.

■ AUTHOR INFORMATION

Corresponding Author

*E-mail: (P.M.A.) ajayan@rice.edu; (A.R.) angel.rubio@ehu.es; (Y.Y.) ysyin@shmtu.edu.

Author Contributions

#These authors contributed equally to this work.

Notes

The authors declare no competing financial interest.

■ ACKNOWLEDGMENTS

P.M.A. acknowledges funding from the Army Research Office through MURI program on novel free-Standing 2D crystalline materials focusing on atomic layers of nitrides, oxides, and sulfides, and the MURI program on graphene supported by the Office of Naval Research. A.R. acknowledges financial support from the European Research Council Advanced Grant DYNamo (ERC-2010-AdG -Proposal No. 267374), Spanish MICINN (FIS2010-21282-C02-01), ACIPromociona (ACI2009-1036), Grupos Consolidados UPV/EHU del Gobierno Vasco" (IT-319-07), the EU project THEMA (Contract Number 228539), and the Ikerbasque Foundation. Y.Y. acknowledges funding from the National Natural Science Foundation of China (51042013, 51003056), the Shanghai City Committee of Science and Technology Project (10170502400), and the National Oceanic Administration Project (201005028-4). J.T.-T. acknowledges the support from PGE and CONACYT (213780).

■ REFERENCES

(1) Geim, A. K.; Novoselov., K. S. The rise of graphene. *Nat. Mater.* **2007**, *6*, 183−191.

(2) Corso, M.; Auwärter, W.; Muntwiler, M.; Tamai, A.; Greber, T.; Osterwalder, J. Boron nitride nanomesh. *Science* **2004**, *303* (5655), 217−220.

(3) Nagashima, A.; Tejima, N.; Gamou, Y.; Kawai, T.; Oshima, C. Electronic structure of monolayer hexagonal boron nitride physisorbed on metal surfaces. *Phys. Rev. Lett.* **1995**, *75*, 3918.

(4) Pacilé, D.; Meyer, J. C.; Girit, Ç. Ö.; Zettl, A. The two-dimensional phase of boron nitride: Few-atomic-layer sheets and suspended membranes. *Appl. Phys. Lett.* **2008**, *92*, 133107.

(5) Ci, L.; Song, L.; Jin, C.; Jariwala, D.; Wu, D.; Li, Y.; Srivastava, A.; Wang, Z. F.; Storr, K.; Balicas, L.; Liu, F.; Ajayan, P. M. Atomic layers of hybridized boron nitride and graphene domains. *Nat. Mater.* **2010**, *9*, 435−430.

(6) Song, L.; Ci, L.; Lu, H.; Sorokin, P. B.; Jin, C.; Ni, J.; Kvashnin, A. G.; Kvashnin, D. G.; Lou, J.; Yakobson, B. I.; Ajayan, P. M. Large scale growth and characterization of atomic hexagonal boron nitride layers. *Nano Lett.* **2010**, *10*, 3209−3215.

(7) Lin, Y.; Williams, T. V.; Connell, J. W. Soluble, exfoliated hexagonal boron nitride Nanosheets. *J. Phys. Chem. Lett.* **2010**, *1*, 277−283.

(8) Coleman, J. N.; Lotya, M. Two-dimensional nanosheets produced by liquid exfoliation of layered. *Science* **2011**, *331*, 568.

(9) Koma, A.; Sunouchi, K.; Miyajima, T. Fabrication and characterization of heterostructures with subnanometer thickness. *Microelectron. Eng.* **1984**, *2*, 129−136.

(10) Nguyen, N. T.; Howe, B.; Hash, J. R.; Liebrecht, N.; Johnson, D. C. Synthesis of $[(VSe_2)n]1.06[(TaSe_2)n]$ superlattices using a hybrid approach: self-assembly of amorphous nanostructured reactants. *Adv. Mater.* **2006**, *18*, 118−122.

(11) Utama, M. I. B.; Belarre, F. J.; Magen, C.; Peng, B.; Arbiol, J.; Xiong, Q. Study with ZnO on muscovite mica substrates. *Nano Lett.* **2012**, *12*, 2146−2152.

(12) Makovicky, E.; Hyde, B. G. *Non commensurate (Misfit) layer structure in:Structure and bonding*; Springer: Herdelberg, 1981; Vol. *46*, pp 101−170.

(13) Li, H.; Cao, J.; Zheng, W.; Chen, Y.; Wu, D.; Dang, W.; Wang, K.; Peng, H.; Liu, Z. Controlled synthesis of topological insulator nanoplate arrays on mica. *J. Am. Chem. Soc.* **2012**, *134*, 6132−6135.

(14) Lin, Q.; Smeller, M.; Heideman, C. L.; Zschack, P.; Koyano, M.; Anderson, M. D.; Kykyneshi, R.; Keszler, D. A.; Anderson, I. M.; Johnson, D. C. Rational synthesis and characterization of a new family of low thermal conductivity misfit layer compounds $[(PbSe)0.99]m(WSe_2)n$. *Chem. Mater.* **2010**, *22*, 1002−1009.

(15) Harris, F. R.; Standridge, S.; Feik, C.; Johnson, D. C. Design and synthesis of $[(Bi_2Te_3)x(TiTe_2)y]$ superlattices. *Angew. Chem., Int. Ed.* **2003**, *42*, 5296−5299.

(16) Cahangirov, S.; Ciraci, S. Two-dimensional C/BN core/shell structures. *Phys. Rev. B* **2011**, *83*, 165448.

(17) Tijerina, J. T.; Narayanan, T. N.; Gao, G.; Rohde, M.; Tsentalovich, D.; Pasquali, M.; Ajayan, P. M. Electrically insulating thermal nano-oils using 2D fillers. *ACS Nano* **2012**, *6*, 1214−1220.

(18) Choi, E. Y.; Choi, W. S.; Lee, Y. B.; Noh, Y. Y. Production of graphene by exfoliation of graphite in a volatile organic solvent. *Nanotechnology* **2012**, *22*, 365601.

(19) Hernandez, Y.; Nicolosi, V.; Lotya, M.; Blighe, F. M.; Sun, Z.; De, S.; McGovern, I. T.; Holland, B.; Byme, M.; Gun'Ko, Y. K.; Boland, J. J.; Niraj, P.; Duesberg, G.; Krishnamurthy, S.; Goodhue, R.; Hutchison, J.; Scardaci, V.; Ferrari, A. C.; Coleman, J. N. High-yield production of graphene by liquid-phase exfoliation of graphite. *Nature Nanotech.* **2008**, *3*, 563−568.

(20) Zhi, C.; Bando, Y.; Tang, C.; Kuwahara, H.; Golberg, D. Large-scale fabrication of boron nitride nanosheets and their utilization in polymeric composites with improved thermal and mechanical properties. *Adv. Mater.* **2009**, *21*, 2889−2893.

(21) Warner, J. H.; Rmmeli, M. H.; Bachmatiuk, A.; Büchner, B. Atomic resolution imaging and topography of boron nitride sheets produced by chemical exfoliation. *ACS Nano* **2010**, *4*, 1299−1304.

(22) Han, W. Q.; Wu, L.; Watanabe, K.; Taniguchi, T. Structure of chemically derived mono- and few-atomic-layer boron nitride sheets. *Appl. Phys. Lett.* **2008**, *93*, 223103.

(23) Lin, Y.; Williams, T. V.; Xu, T. B.; Cao, W.; Elsayed-Ali, H. E.; Connell, J. W. Aqueous dispersions of few-layered and monolayered hexagonal boron nitride nanosheets from sonication-assisted hydrolysis: critical role of water. *J. Phys. Chem. C* **2011**, *115*, 2679−2685.

(24) Dean, C. R.; Young, A. F.; Meric, I.; Lee, C.; Wang, L.; Sorgenfrei, S.; Watanabe, K.; Taniguchi, T.; Hone, J. Boron nitride substrates for high-quality graphene electronics. *Nat. Nanotechnol.* **2010**, *5*, 722−726.

(25) Meyer, J. C.; Chuvilin, A.; Algara-Siller, G.; Biskupek, J.; Kaiser, U. Selective sputtering and atomic resolution imaging of atomically thin boron nitride membranes. *Nano Lett.* **2009**, *9*, 2683−2689.

(26) Alem, N.; Erni, R.; Kisielowski, C.; Rossell, M. D.; Gannett, W.; Zettl, A. Atomically thin hexagonal boron nitride probed by ultrahigh-resolution transmission electron microscopy. *Phys. Rev. B* **2009**, *80*, 155425.

(27) Arenal, R.; Kociak, M.; Zaluzec, N. J. High-angular-resolution electron energy loss spectroscopy of hexagonal boron nitride. *Appl. Phys. Lett.* **2007**, *90*, 204105.
(28) Azevedo, S.; Kaschny, J. R.; de Castilho, C. M. C.; de Brito Mota., F. A theoretical investigation of defects in a boron nitride monolayer. *Nanotechnology* **2007**, *18*, 495707.
(29) Ferrari, A. C.; Meyer, J. C.; Scardaci, V.; Casiraghi, C.; Lazzeri, M.; Mauri, F.; Piscanec, S.; Jiang, D.; Novoselov, K. S.; Roth, S.; Geim, A. K. Raman spectrum of graphene and graphene layers. *Phys. Rev. Lett.* **2006**, *97*, 187401.
(30) Sun, Z.; Yan, Z.; Yao, J.; Beitler, E.; Zhu, Y.; Tour, J. M. Growth of graphene from solid carbon sources. *Nature* **2010**, *468*, 549−552.
(31) Narayanan, T. N.; Kumar, D. S.; Yoshida, Y.; Anantharaman, M. R. Strain induced anomalous red shift in mesoscopic iron oxide prepared by a novel technique. *Bull Mater. Sci.* **2008**, *31*, 759−766.
(32) Miyamoto, Y.; Rubio, A.; Louie, S. G.; Cohen, M. L. Electronic properties of tubule forms of hexagonal BC_3. *Phys. Rev. B* **1994**, *50*, 18360.
(33) Wada, Y. K.; Yap, M.; Yoshimura, Y.; Mori, T. S. The control of B-N and B-C bonds in BCN films synthesized using pulsed laser deposition. *Diamond Related mater.* **2010**, *9*, 620−624.
(34) Caretti, I.; Jiménez, I.; Albella, J. M. BCN films with controlled composition obtained by the interaction between molecular beams of B and C with nitrogen ion beams. *Diamond Relat. Mater.* **2003**, *12*, 1079−1083.
(35) Xu, S.; Ma, X.; Sun, M. Synthesis of boron carbonitride films by plasma-based ion implantation. *Key Eng. Mater.* **2007**, *353*−*358*, 1850−1853.
(36) Chen, J. H.; Jang, C.; Xiao, S. D.; Ishigami, M.; Fuhrer, M. S. Intrinsic and extrinsic performance limits of graphene devices on SiO_2. *Nat. Nanotechnol.* **2008**, *3*, 206−209.
(37) Giannozzi, P.; et al. http://www.quantum-espresso.org.
(38) Marini, A.; et al. *Comp. Phys. Comm.* **2009**, *180*, 1392.
(39) Bokdam, M.; Khomyakov, P. A.; Brocks, G.; Zhong, Z.; Kelly, P. J. Electrostatic doping of graphene through ultrathin hexagonal boron nitride films. *Nano Lett.* **2011**, *11* (11), 4631−4635.
(40) Dean, C. R.; Young, A. F.; Meric, I.; Lee, C. L.; Wang, S.; Sorgenfrei, K.; Taniguchi, T. W.; Kim, P.; Shepard, K. L.; Hone, J. Boron nitride substrates for high-quality graphene electronics. *Nat. Nanotechnol.* **2010**, *5*, 722.
(41) Xue, J.; Yamagishi, J. S.; Bulmash, D.; Jacquod, P.; Deshpande, A.; Watanabe, K.; Taniguchi, T.; Jarillo-Herrero, P.; LeRoy, B. J. Scanning tunnelling microscopy and spectroscopy of ultra-flat graphene on hexagonal boron nitride. *Nat. Mater.* **2011**, *10*, 282.
(42) Decker, R.; Wang, Y.; Brar, V. W.; Regan, W.; Tsai, H.; Wu, Q.; Gannett, W.; Zettl, A.; Crommie, M. F. Local electronic properties of graphene on a BN substrate via scanning tunneling microscopy. *Nano Lett.* **2011**, *11*, 2291.
(43) Lui, C. H.; Li, Z.; Mak, K. F.; Cappellutti, E.; Heinz, T. F. Observation of an electrically tunable band gap in trilayer graphene. *Nat. Phys.* **2011**, *7*, 944−947.
(44) Wirtz, L.; Marini, A.; Rubio, A. Excitons in boron nitride nanotubes: dimensionality effects. *Phys. Rev. Lett.* **2006**, *96*, 126104.
(45) Trevisanutto, P.; Holzmann, M.; Cote, M.; Olevano., V. Ab initio high-energy excitonic effects in graphite and graphene. *Phys. Rev. B* **2010**, *81*, 121405.